PRELIMINARY SIZING OF A LOW-ALTITUDE AIRSHIP INCLUDING ION-PLASMA THRUSTERS

Carlo E.D. Riboldi[1], Marco Belan[1], Stefano Cacciola[1], Raffaello Terenzi[1], Stefano Trovato[1], Davide Usuelli[1] & Giuseppe Familiari[1]

[1]Department of Aerospace Science and Technology, Politecnico di Milano - via La Masa, 34 - 20156 Milano, Italy

Abstract

The adoption of ion-plasma thrusters on airships, representing the scope of the research project IPROP, promises to offer a stark reduction in the complexity of stratospheric surveillance platforms, thus reducing the rate of failures, increasing the time between overhauls (TBO), and in turns extending the mission time. A first practical demonstration of this propulsive technology, which has been applied in aeronautics only sporadically, is a planned milestone in this research project, together with the setup of suitable design and sizing procedures for airships coping with the specificity of this propulsion technique. Such design procedures are in the focus of the present contribution. Besides introducing these algorithms from a conceptual standpoint, the present work reports sizing results and considerations obtained from the application of these procedures to a specific demonstration mission, yielding the preliminary design and sizing data of a flying demonstrator running on ion-plasma thrusters.

Keywords: ion-plasma thruster; airship; LTA; preliminary sizing; demonstrator; low altitude; IPROP

1. Introduction

Thanks to their inherently longer endurance compared to fixed-wing and rotary-wing flying craft, lighter-than-air platforms are currently gaining interest as a cheaper, more versatile and more easily-deployable alternative to space satellites [1, 2, 3] and to unmanned flying vehicles (UAV) for prolonged surveillance missions (which are entering commercial operation in these years [4]).

Similar to fixed-wing aircraft [5], the preliminary sizing phase of an airship is crucial in orienting the latter, more detailed stages of the design. Despite being less documented with respect to the case of fixed-wing platforms, some detailed preliminary design and sizing techniques have been described in the literature for airships. Among those, the most widely accepted [6, 7] devote much attention to the adoption of dynamic envelopes, so as to produce an airship capable of obtaining a significant lift component from motion (instead of buoyancy), as well as to the setup of technological regressions for standard components, for instance linking weight and power loss efficiency to the length of electric cables, or the stress within the envelope skin to the inflation pressure. Comparatively less attention is dedicated to the inclusion of non-fuel based propulsion systems. On the other hand, trying to cope with the need to support the concept of a high-altitude airship (HAA) capable of a rapid deployment to an altitude of 18-25 km via a missile vector (the satelloon concept, a particular declination of the high-altitude pseudo-satellite mission, or HAPS), a preliminary sizing technique largely employing electric propulsion and solar energy harvesting has been also presented in the literature [8]. In the latter, a weight-optimal approach is also introduced, such to output a preliminary sizing not just capable of energetically self-sustaining for an assigned time and altitude, thus covering the mission requirements, but also optimizing design weight, hence potentially reducing the need for a heavier missile launch platform, and bearing an all-around beneficial effect on power and energy requirements.

Besides documenting preliminary design techniques, available results from theoretical or simulation analysis and from the field [7, 8, 2, 9, 10], have highlighted a strong sensitivity of the design point (typically defined mainly in terms of envelope volume, thickness and inflation pressure, energy storage requirements, propulsion system and detailed weight breakdown for all components) with respect to the choice of some technological parameters (e.g. assumptions on the efficiency and mass associated to power lines) and mission specifications, in particular altitude and geographical location of the target deployment, especially when solar harvesting is employed [8, 11].
In order to increase dependability and the level of autonomy of LTAs for longer missions, in a similar fashion to winged aircraft the reduction of complexity is generally a design goal. On LTAs, a first reduction in complexity comes with the electrification of the propulsion system, which thanks to the very high power-to-weight ratio of electric motors, allows to de-localize the thrusters (i.e. the motor/propeller assemblies) on-board. This in turns enables the potential deletion of deflectable surfaces on the tail, thus removing the need for actuators and related power lines. Despite making control design potentially trickier in forward flight conditions, a thrust-controlled airship is inherently capable of more control authority in hovering and near-hovering flight [12, 13, 14].
To further reduce manufacture complexity, while also making the platform less detectable, which is relevant especially for surveillance missions, removing movable components altogether from the platform is an interesting goal. A propulsive technology which enables pursuing this achievement is that of ion plasma thrusters [15, 16, 17]. Based only on clusters of emitters and collectors configured in a pre-defined and fixed geometrical configuration, ion-plasma thrusters feature no movable parts. While generally limited in terms of overall thrust, these thrusters potentially represent a good match for airships, since these platform do not rely on thrust for staying aloft. They also provide a good steering and attitude control capability both in dynamic and near-hover conditions.
The application of ion plasma thrusters in aeronautics is still in an early stage [18], and a thorough assessment of its feasibility is in the focus of the research project `IPROP` (Ionic PROPulsion in Atmoshpere [19]), which is currently investigating this concept at a theoretical, subsystem and flying prototype level. Where specific issues related to the development of the thruster unit will be tackled through the study of the physics and technology underlying it, the development of a low-altitude flying airship demonstrator and of a detailed high-altitude airship concept are among the goals of the project as well.
The present contribution analyzes and showcases the first investigation results connected with the design of a low-altitude airship featuring ion plasma thrusters. The structure of the paper is as follows. A quick review of the general methodology applied to the design of airships of arbitrary scale, developed at DAER-Politecnico di Milano and wrapped in the preliminary sizing suite `Morning Star` [8], will be provided first. Then a description of the technology of ion-plasma thrusters will be featured, considering the current level of technology development within the `IPROP` project. In particular, the focus of the description will highlight those quantities which need to be assigned in the context of a preliminary sizing procedure. With these notions, a new version of the sizing methodology, extended with respect to the baseline one by accounting for the need to concurrently size up the airship for a specific mission and the ion-plasma thrusters intended to propel it, will be presented in detail. This sizing procedure will be then applied to the specific case of the preliminary sizing of a low-altitude unmanned airship demonstrator, among the planned milestones of the `IPROP` project, capable of performing a complete short-term mission in proximity to the ground, and powered by ion-plasma thrusters only.

2. Airship sizing methodology

Drawing on the preliminary experience of the authors in drafting a sizing technique for HAAs featuring electric propulsion (in particular, electric propellers) [8], in this contribution a procedure for low-altitude airships (LAAs) with that type of propulsion system on board is introduced first. This is based on two geometric parameters only as independent variables, namely the actual length L_r of the airship envelope and the fineness ratio FR, customarily defined [7] as the ratio between the length L_r and the top diameter $2R$ of the envelope. These can be solved numerically as unknown parameters in an automated fashion, according to an optimal procedure targeting the overall weight of the platform W. The corresponding sizing procedure will be outlined in the following, illustrating at first the sizing

loop, i.e. a procedure allowing to compute the weight break-down corresponding to a specific choice of the geometrical parameters just mentioned, as well as to a set of assigned and constant values for a set of technological quantities, and a guessed value of the overall weight W^{guess}, employed to start the loop. Subsequently, the structure of an optimizer such to manipulate the geometrical parameters so as to steer the sizing solution towards minimum weight will be briefly described.

2.1 Sizing loop procedure

Considering a baseline airship propelled by electric propulsion, the following sizing loop can be employed to compute the airship weight break-down corresponding to the assignment of the independent parameters L_r and FR. In a different fashion from previous works by the authors [8], in view of the application of the design methodology to the case of a low-altitude airship, solar cells have not been considered as a source of power in the design, on account of the relatively low irradiance next to the ground, and of the mild endurance requirement of a demonstration mission. Therefore, the energy required to cover the mission shall be stored in the batteries only. Similarly, in view of the application of the proposed procedure to the sizing of a low-altitude demonstrator, components allowing to manage a change of lifting gas volume as a result of an altitude change (i.e. typically ballonets) are not considered in the design.

2.1.1 Analysis of the mission profile

The target of this section of the sizing algorithm is that of computing the thrust and power required along the mission, and in particular the corresponding peak values, as well as the energy required to fly the mission profile.

For preliminary design purposes, a mission profile can be assigned according to an idealization of a mission, including in particular climb, cruise and descent phases. In turn, the assignment of such profile can be reduced to the specification of a cruise altitude h_{cr}, climb and descent angles γ_c and γ_d, as well as inertial velocity values along the corresponding three mission legs, respectively V_c, V_{cr} and V_d. Furthermore, the endurance in cruise τ_{cr} is another parameter often defined by the designer (in particular for a station-keeping mission, or in the case of the technological demonstration mission at hand), whereas the values of the time for the climb and descent phases are a result of a kinematic computation based on speed, angle and target altitude (i.e. parameters already specified).

The altitude profile is employed to obtain corresponding values of the thermodynamic state of the atmosphere along the mission, in particular the density ρ_{air}, pressure P_{air}, temperature T_{air}, viscosity ν_{air}, as well as the velocity and direction of the average wind at altitude.

To increase accuracy, the computation of these quantities, similar to the flight mechanics computations to follow, is carried out in the nodes of a suitably time-discretized mission profile.

The core step in the computations related to the mission profile is the definition of the drag force associated to the flight along its evolution. The values of L_r and FR allow to define the overall geometry of the hull, thus producing its volume Vol, as well as the areas of the frontal and side sections, A_f and A_s respectively. In this study, a bi-ellipsoidal shape has been adopted, as proposed by the National Physics Laboratory (NPL) [20] model. This shape is based on two semi-ellipsoids, jointed at the level of the maximum thickness location, with semi-major axes a_1 and a_2 such that $a_2 = \sqrt{2}a_1$, and semi-minor axis b. A complete analytic description of the corresponding surface can be obtained from the cited parameters L_r and FR.

Those geometrical quantities, together with air viscosity ν_{air} and airspeed V, allow to obtain an estimation of the component of the drag coefficient $C_{D,0}$, independent from the value of the lift force, through regressions [7].

Furthermore, by knowing the volume Vol, it is possible to compute the buoyancy force B from the value of ρ_{air} at any point along the mission profile by definition, since $B = \rho_{air} Vol$. This in turns allows to complete the computation of drag force at any time node, starting from the satisfaction of the equilibrium equation normal to the trajectory,

$$(W - B)\cos\gamma = L \tag{1}$$

which can be applied in climb, cruise and descent, respectively with $\gamma = \gamma_c$, $\gamma = 0$ and $\gamma = \gamma_d$. Employing a guessed value of the airship weight W^{guess}, the expression in Eq. 1 can be exploited to obtain

the value of lift for every time node, thus correspondingly the lift coefficient and the drag-due-to-lift component through a typical parabolic polar, writing

$$C_D = C_{D,0} + KC_L^2 = C_{D,0} + K\left(\frac{L}{\frac{1}{2}\rho_{air} Vol^{\frac{2}{3}} V^2}\right)^2. \tag{2}$$

In Eq. 2 the value of coefficient K is obtained from a semi-empirical model [7], once more on the base of the airship geometrical parameters already specified or computed. The value of the airspeed V represents the airspeed intensity specified for a given node along the mission profile. Therefore, it is obtained from the knowledge of the local wind intensity at the specific altitude of the node, and from the value of the inertial velocity in the corresponding leg of the mission.
With a knowledge of the drag coefficient, it is possible to compute the corresponding drag force intensity D at any time node along the profile. Correspondingly, a value of the power required can be obtained by definition as $P_r = DV$.

2.1.2 Estimation of the break-down of take-off weight

This part of the sizing algorithm aims at computing the weight pertaining to most components of the airship design laid out, i.e. the break-down of the overall weight of the machine. Correspondingly, an estimation of the weight of the airship can be obtained at the end of this step, by putting together all components of the break-down.
For obtaining an estimation of the weight of most components of the airship, it is typically possible to deploy models either retrieved from technological regressions or defined through the direct assignment of some technological parameters.
According to the hypothesis of a purely battery-powered platform, among the most relevant weight components are typically those listed in the following.

- *Batteries*. The weight of the batteries is a result of the computations in section 2.1.1. In particular, from the knowledge of the profile of power versus time required along the mission, it is possible to compute the peak required power $P_{r,\max}$. From the same power profile it is also possible to compute the value of total energy E required for covering the mission, through a direct numerical integration over time of the time history of power required. From the knowledge of these quantities, it is possible to carry out the sizing of the battery, according to the most stringent requirement, so that

$$W_{bat} = \frac{1}{\eta_d \eta_m \eta_p} \max\left(\frac{E}{e_{bat}}, \frac{P_{r,\max}}{p_{bat}}\right). \tag{3}$$

  In Eq. 3 the values of e_{bat} and p_{bat} represent the specific energy and power of the battery, η_d the battery discharge efficiency, η_m the efficiency of the motors and η_p the efficiency of the propeller. The values of e_{bat} and p_{bat} are typically related to one another, through a specific choice of the chemistry of the battery [21].

- *Motors and gondola*. From the knowledge of the characteristics of the power profile along the mission, it is possible to obtain motor data matching the requirements, typically from industrial catalogs or from corresponding regression models available for typical electric motors [21, 22, 23], thus yielding a corresponding value of weight W_m. Clearly, this part will be substantially emended when considering ion-plasma thrusters (see section 3.).

  In the layout of an unmanned airship, it can be assumed to have the payload, the power storage (associated to W_{bat}), power management and signal conditioning systems (W_{el}), all stored in the gondola. The mass and weight W_{gon} of this typically light structure (at least for non-rigid airships) is therefore proportional to the weight of the components it carries [7].

- *Lifting gas*. The weight of the buoyant component of the airship is composed of the weight of the envelope and that of the lifting gas. A knowledge of the mass of lifting gas is obtained based on the envelope volume Vol, and from the need to satisfy a minimum pressure differential

$\Delta\bar{P}_{in-out}$ between the inside and outside of the envelope. This requirement, including the value of $\Delta\bar{P}_{in-out}$, is due to the need to guarantee an acceptable level of consistency of the shape of the envelope, accounting for wind gusts and disturbances, attained in practice by stiffening the envelope through inflation. Starting from a knowledge of the outside pressure at altitude, typically higher at take-off than at the increasingly higher altitude values reached during the flight, it is possible to compute the value of the inside pressure by imposing the required pressure differential, thus obtaining the inflation pressure as

$$P_{in} = P_{air} + \Delta\bar{P}_{in-out}. \tag{4}$$

Given the volume Vol, temperature T_{air} (assumed equal to that of the lifting gas) and pressure P_{in}, it is possible to compute the mass and weight of the lifting gas, W_{lg}.

- *Envelope skin*. Given the mass and inflation pressure of the lifting gas, computed at the previous point at a specific altitude (typically corresponding to take-off), it is possible to compute the pressure differential between the lifting gas P_{in} and the atmosphere P_{air} along the mission profile, accounting in particular for the evolution of the altitude and consequently of the outside pressure. For non-rigid airships experiencing a significant altitude change during a mission, a system of ballonets is typically employed to constrain the pressure differential within a reasonable value, so as to avoid an increase in the stress within the envelope skin, at least up to a certain target altitude. However, for the case of a low-altitude demonstrator, as stated in the introduction to the present section 2.1, ballonets have not been taken into account in the design procedure, in consideration of the reduced altitude excursion expected along the mission. Consequently, a change with altitude in the stress within the skin of the envelope is implicitly accepted. While on the one hand this puts a technological limit on the target altitude of the mission (dictated by a condition where the top stress which the skin material can sustain $\bar{\sigma}_{\max}$ is matched by the value of the stress achieved in practice), on the other it reduces the overall weight and complexity of the platform.

  In a computational perspective, having evaluated the pressure differential along the mission profile, it is possible to find its maximum $\Delta P_{in-out_{\max}}$, and based on statistical regressions [7], also a corresponding value of the top stress within the skin $\sigma_{\max}$. The latter can be turned into a corresponding mass and weight W_{env} of the envelope, again employing technological data from an assumed envelope material (since $\sigma_{\max}$ is proportional to the skin thickness, which in turns produces a certain mass, given the overall volume Vol contoured by the skin). Notably, from the knowledge of the weight component W_{env} it is possible to compute the additional weight of inner septa and tension cables (wrapped in the term W_{str}), which completes the structural weight of the envelope, as well as that due to the tail fins and corresponding bracers (defining W_t). The latter can be estimated at this level, starting from a knowledge of the size of the tail, in turn estimated through regression models based on pre-existing technological data [8].

Following the definition of all the components in the break-down of the total weight of the airship, it is possible to assemble the latter by simple sum, yielding

$$W = W_{env} + W_{lg} + W_{bat} + W_m + W_{el} + W_{gon} + W_{str} + W_t + W_{pl}, \tag{5}$$

where the component W_{pl} represents the weight of the payload, which is known to the designer, and in the case of a demonstrator may be constituted by a set of sensors and a corresponding recording unit (including a video recorder, if needed). For the demonstrator at hand, care will be taken to keep the weight of the payload to a minimum, while obtaining a set of measurements such to allow a correct piloting of the machine.
Starting from a guess weight W^{guess}, the sizing loop can be iterated after W has been obtained correspondingly, through all the passages described in section 2.1, leading to the estimation in Eq. 5. Following iteration, the sizing loop will converge to a final weight W corresponding to the current choice of the design parameters L_r and FR, beside all the technological specifications required for the completion of the procedure.

2.2 Weight-optimal design solution

The selection of the airship length L_r and fineness ratio FR, yielding a value of the weight W according to the sizing loop and Eq. 5, can be delegated to an automatic optimal solver, which steers the independent parameters L_r and FR, so as to minimize W itself. The optimization process can be set up considering also a set of bounds on the optimization parameters, as well as inequality constraints, functions of the the latter.

In the present implementation, lower and upper bounds on both the length L_r and fineness ratio FR have been specified to draw the optimizer within an area of technologically realistic solutions, in particular avoiding excessively short or long envelopes, and disproportionately slender or blunt shapes. Where the first bound is due mostly to manufacture constraints, as said, the latter (on FR) is also due to the fact that the aerodynamic estimations employed for the analysis of the mission profile result from the adoption of slender body theory [24], which is acceptably accurate only for a certain range of that parameter.

The inequality constraints considered in this process are two, namely one on the integrity of the envelope, and the other on the self-sustainability of the airship in flight. The sizing of the airship considers a specific material, which is associated to a given value of $\bar{\sigma}_{\max}$. The computation of $\sigma_{\max}$ within the sizing loop (see section 2.1.2) allows to populate the inequality p_1

$$p_1: \quad \sigma_{\max} - \bar{\sigma}_{\max} < 0, \tag{6}$$

which represents a technological limit to avoid a potential damage to the envelope skin. The second constraint can be written as

$$p_2: \quad BR - \frac{B_{h_{cr}}}{W} < 0, \tag{7}$$

wherein it should be noted that the target buoyancy ratio BR is an assigned design parameter, whereas weight W and buoyancy $B_{h_{cr}}$ are computed respectively from the break-down of weights (Eq. 5) and from the volume Vol of the envelope and the density of air ρ_{air} at the top altitude h_{cr} in the mission profile (since this is the condition typically corresponding to the lowest buoyancy along the mission profile, making the satisfaction of Eq. 7 more challenging to achieve).

A schematic representation of the sizing loop and of the weight-optimal algorithm are shown in Fig. 1.

A corresponding analytic description of the optimal problem can be given as

$$\min_{L_r, FR} W \; s.t. \; \{p_1, p_2\}. \tag{8}$$

Similar to previous works by the authors [8, 11], this problem appears generally very regular, thus allowing to safely seek for a solution by deploying a gradient-based optimization method.

3. Including ion plasma thrusters in the design procedure

The sizing loop and optimal-weight-seeking algorithm presented in the previous section 2. can be largely retained when dealing with ion-plasma thrusters, instead of standard electric motor and propeller assemblies. However, in order to accurately describe what are the modifications required to the baseline design procedure when including this novel type of thrusters on board, a quick review of their geometry and associated technological parameters is required. This will be presented in the next subsection, followed by the proposed corresponding amendment to the design methodology.

3.1 Ion-plasma thrusters for airships

Ion-plasma thrusters exploit the formation of ionized plasma from air, and its acceleration between two electrodes set at a distance from one another and subject to an assigned voltage differential. A couple of such electrodes, composing the basic nucleus of the thruster, is made of an *emitter* and a *collector*. Clusters of emitters and collectors, geometrically arranged in parallel (with emitters to the front and collectors to the back), allow to upscale the propulsive yield of a single couple while retaining most of the power signal conditioning apparatus and load-bearing structure, thus allowing to set-up a thruster in this fashion.

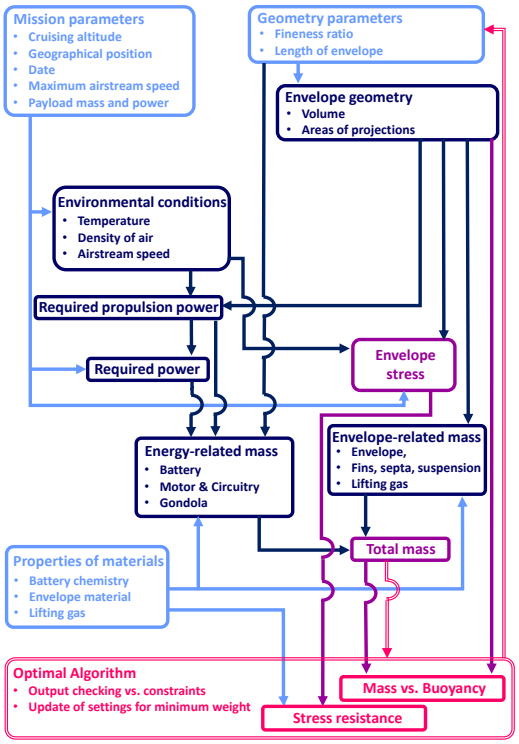

Figure 1 – Preliminary sizing algorithm for airships with standard propulsion. Sizing loop and weight optimization.

Current research efforts [15, 16, 17] (and the most recent developments within project IPROP) are investigating the properties of these thrusters, with respect to the geometrical characteristics of the setup. In particular, the number of emitters and collectors (which might not be defined according to a 1:1 rule in a thruster, but may be arranged in a way such that more than one emitter feeds a single collector), their mutual positioning and distances, the lofting and sizing of the emitters and (especially) of the collectors, all bear an impact on the performance of the resulting thruster. Concerning the shaping of collectors, a smart way of obtaining good aerodynamic and electrical properties for this component has been proved to be the adoption of thin airfoils (the target for aerodynamic performance, in particular, is that of minimizing drag). Therefore, where emitters are typically thin wires with no special aerodynamic property, collectors need more care in terms of manufacture, choice of the material (so as to optimize weight vs. strength), and construction strategy as well (for instance, they might be built either as hollow structures similar to typical aircraft empennages, or conversely as filled structures).

To the aim of setting up a computational procedure able to manipulate the variables which assign the geometry of the thruster according to an automated algorithm, the definitions in Fig. 2 can be provided. Considering a single emitter-collector couple in that figure, c is the chord of the collector, d is the distance between the emitter and the leading edge of the collector. The sum of these distances gives $l = c + d$. Considering a cluster of more emitters and collectors forming a thruster, the distance between two adjoining collectors is defined as Δs, whereas the total radial extension of the thruster is s, and it can be obtained from the number of collectors N_c and the distance Δs as $s = (N_c - 1)\,\Delta s$.

The length l and height s define two components of the overall dimensions of the thruster. The last one, namely a measure of width w, is bound to the span of the collector. Due to the physics underlying the plasma-based propulsive effect, it is typical to have a minimum size constraint, which comes in terms of minimum gap d between the emitters and collectors, a minimum span w to reduce boundary effects close to the tips of the collectors, as well as minimum radial and longitudinal extensions (respectively s and l) of the overall thruster.

The supporting structure of the thruster is composed of two side plates, and of load-bearing rods connecting them. Thanks to the low general values of forces involved, a light material can be employed for the supporting structure, like styrofoam or similarly cheap, easily machinable and 3D-printable

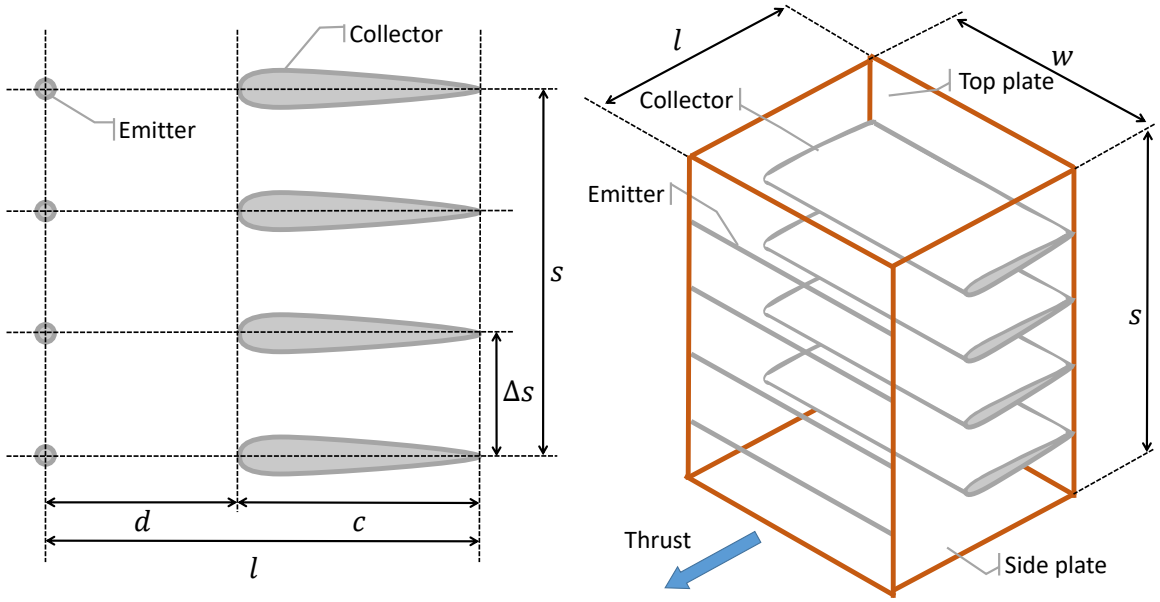

Figure 2 – Schematic representation of an ion-plasma thruster, defining some characteristic geometrical parameters. Left: side view. Right: three-quarters view.

material.

The thruster is electrically fed, with voltage employed for regulating the intensity of thrust. The manipulation of electrical variables requires the employment of specific electric components, including a voltage booster. Typically employed out of the aeronautical domain, existing realizations of this component feature rather penalizing weight performance. However, novel and more performing exemplars of this technology are under development within project IPROP, to allow an easier adoption of this component on flying machines.

In terms of performance, similarly to the domain of turbomachinery, it is typical to define as characteristic figures a thrust-over-frontal area ratio $\frac{T}{A_m}$, thrust-over-weight $\frac{T}{W_m}$ and thrust-over-volume $\frac{T}{V_m}$. Furthermore, a power efficiency measure can be defined through the parameter $\frac{T}{P_m}$, where P_m is the power flow required from the electrical system to produce the corresponding thrust. From experiments, figures have been obtained and characterized for all these quantities within project IPROP, according to the general layout of the proposed implementation.

The material arrangement of ion-plasma thrusters on airships is currently a matter of investigation. Promising solutions have been presented in the literature [17], up to now set up mostly considering the advantages and shortcomings of the mutual placement of multiple thrusters in a stream-wise direction on the side of the envelope. The interaction of multiple stream-wise aligned thrusters - which in that configuration take the name of *longitudinal stages* - is still under investigation [25, 26], and results currently available appear to indicate the existence of constraints on the minimum longitudinal distance between the stages, and a maximum recommendable number. This is explained by a significant increase in drag, besides thrust, associated to an increase in the number of stages. This in turns produces a progressively less steep increase of net thrust per additional stage, when the number of longitudinal stages is increased.

An option considered in the present study is that of arranging multiple thrusters sharing the frontal area, but set sufficiently apart in a longitudinal direction to allow considering the interaction between stream-wise aligned thrusters negligible. Where the study of the detailed lofting of multiple thrusters on board the airship has not been included in the present work, the adoption of this layout allows some flexibility in the longitudinal placement of the thrusters, which is of great relevance for longitudinal balancing in static or near-hover conditions [12, 14], as well as for maneuverability. These static balance and dynamics aspects, which of course constrain the positioning of thrusters (as well as that of stages, in a stream-wise close-coupled multi-stage arrangement), will be in the focus of further studies within IPROP.

3.2 A sizing methodology for ion-plasma thrusters on airships

From the standpoint of a sizing algorithm, the adoption of ion-plasma thrusters requires the definition of a series of geometrical and technological parameters, while leaving one (or a set) of design parameters free to tune, so as to cope with design requirements. The actual sizing value of this parameter (or this set of parameters) shall be defined based on the same type of requirement leading to the adoption of a certain electric motor in the baseline procedure (section 2.), namely the need to satisfy equilibrium conditions along the mission profile.
A difference between the sizing of ion-plasma thrusters and electric motor/propeller assemblies lies in the fact that the former, where scaled up in size to increase thrust, tend to concurrently increase drag, mostly due to the side plates and thruster cover, forming a nacelle for the thrusters, similar to ducted fans or jet engines. Such increase in drag needs to be assessed, so as to avoid over-estimating the advantage of increasing the size of the thruster components on net thrust.
In the proposed sizing methodology, the amendment due to the adoption of ion-plasma thrusters is included at the level of the estimation of the thrust required for the mission profile (section 2.1.1).

3.2.1 Assigned architectural and technological parameters

Firstly, it is assumed to work with assigned data concerning the following aspects.

- Number of thrusters N_t. Thrusters are also hypothesized to be all similar in construction, and arranged in a stream-wise direction without any interaction between them.
- General arrangement of the thrusters. According to the topology presented in Fig. 3, it is assumed that the thrusters are placed on the lower half of the airship, for obvious balance reasons (center of buoyancy above the center of gravity). Their number at a certain longitudinal section, $N_{t,l}$, is assigned as well, and such that the number of longitudinal stations N_l multiplied by that of the stages per station gives $N_t = N_l N_{t,l}$.

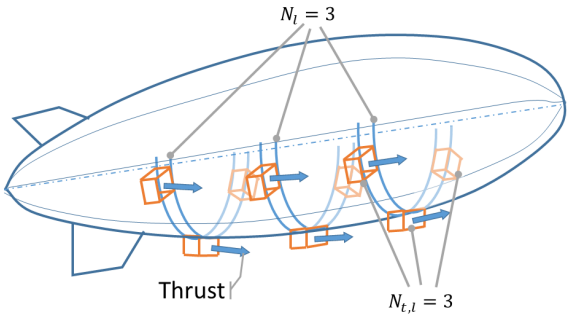

Figure 3 – Basic working topology adopted in the design algorithm.

Of course, the actual specific positioning of the thrusters on board will have an impact on free dynamics (through the corresponding positioning of the center of gravity and the values of the components of the inertia tensor) and controlled response of the airship. However, this level of detail will be dealt with through an analysis of lofting (further on within project IPROP), which is triggered by the preliminary sizing presented in this work.

- Geometrical features of each thruster. In particular, referring to Fig. 2, quantities l and s are known (they are currently being empirically optimized based on purpose-designed testing campaigns, currently being carried out at Politecnico di Milano employing also the wind tunnel). Conversely, the width w of the thrusters is not assigned.
- Thrust-to-frontal area. The value of the ratio $\frac{T}{A_m}$ is considered an assigned constant (similar to geometrical characteristics of the thruster, experimentation targeting the optimization of this value through a trial and error procedure on the thruster configuration is well underway within project IPROP). This relevant assumption is supported by the adoption of a certain geometry and general arrangement of the components within the thrusters (e.g. the relative numbers and

positioning of emitters and collectors, the sizing of the basic components like c, d and Δs, etc.). When these quantities are assumed to be set and not subjected to changes, a linear scalability can be reasonably hypothesized when altering the frontal area of the thruster with respect to a baseline, so that the value of the ratio $\frac{T}{A_m}$ remains constant. In particular, the width w of the thruster has been left free to change, and it is such to produce $A_m = ws$.

- Thrust-to-power. The ratio $\frac{T}{P_m}$ is a measure of the efficiency of the thruster, and it might bear an impact on the actual value of power required from the electrical system (and batteries in particular).

As can be argued from the previous listing, the geometry of a single thruster has been assigned except for the value of the width w, which in turns is associated to a different value of the thrust available from that thruster, obtained multiplying A_m by $\frac{T}{A_m}$.
Furthermore, the side area of the thrusters, defining the area of their nacelle exposed to the airstream and contributing to drag, is assigned only when the value of w is known.

3.2.2 Amendments to the baseline sizing procedure

As can be argued from the previous paragraph, the sizing of ion-plasma thrusters according to the parameters prescribed as constant input, can be reduced to the definition of the width w. Within the sizing loop proposed for airship sizing in the baseline scenario (section 2.), it is possible to carry out the computation of this additional parameter, in a way such to satisfy equilibrium along the mission profile. This is conceptually similar to the baseline case of the electric motor/propeller assembly.
However, a significant difference with respect to the baseline case is in the relationship between the thruster size (hence its nominal thrust) and drag. As explained in the introduction to this section, at the level of the computation of the drag coefficient C_D, an additional component due to the presence of the nacelles of the thrusters has to be taken into account. To this aim, an inner iterative loop where the value of w is solved has been envisaged as follows:

1. Compute the drag associated to the baseline airship, without any additional component and for the entire mission profile (as explained in section 2.).

2. Assign a guess value of w.

3. Complete the assignment of the geometry of the propulsive configuration. This requires computing the front area $A_m = ws$ of each of the N_t thrusters, as well as the area of the side surface of the nacelle, which can be obtained as $A_s = (w+2s)l$, on account of the fact that the nacelle can be assumed to be composed by two side plates of length s and a top plate of length w.

4. Estimate the additional drag due to the nacelles. This step can be performed based on a model of the nacelle sides as flat plates. The drag coefficient of the plate is obtained as a function of the relative velocity and viscosity of air, and of the length of the plate, which compose the Reynolds number.

5. Multiply the drag obtained for one nacelle by N_t to obtain the total additional drag ΔD_m, so that for each node along the mission profile it is possible to compute

$$D_{tot} = D + \Delta D_m. \tag{9}$$

   From this series of values, the maximum drag encountered over the mission as $D_{tot,\max}$ can be computed.

6. Compute the required thrust-to-frontal area ratio for a single thruster. This can be obtained as

$$\left(\frac{T}{A_m}\right)_{req} = \frac{D_{tot,\max}}{N_t A_m}. \tag{10}$$

7. Compare the so-obtained thrust-to-frontal area ratio with the assigned technological specification $\frac{T}{A_m}$.

Based on the outcome of the comparison at point 7, steps from 2 to 7 shall be repeated updating variable w until convergence. Upon reaching convergence, the sizing of the thrusters will be such that their thrust will be able to balance the requirements of the mission, accounting for the drag penalty due to the nacelles.
As a remark, it should be noted that the drag associated to the stream flowing within the thrusters has not been accounted for explicitly. This is due to the fact that the $\frac{T}{A_m}$ figure specified for a certain ion-plasma thruster construction represents a *net thrust*. This is in accordance with what is typically done to provide the characteristic performance of any thruster (e.g. the thrust figure typically specified for a jet engine is not such that the drag of the flow blowing through the compressor and turbine vanes needs to be taken away from it to get the actual thrust).
Once the inner sizing loop producing the geometry and thrust of the propulsive system has been assigned, the corresponding mass can be assessed, in order to amend the computation of the weight break-down within an optimal design procedure, as presented in section 2.1.2. The weight components associated to the ion-plasma thruster can be listed as follows:

- *Wires employed as emitters*. Due to their very limited diameter, these components are associated to a negligible weight.
- *Collectors*. Depending on the material employed and structural sizing (i.e. hollow or filled structure), the weight may vary significantly.
- *Load bearing structure*. Thanks to the relatively low value of force exerted by each thruster, its load bearing structure can be manufactured with relatively light and flexible material. The cage structure naturally resulting from the setup of this type of thruster allows to obtain overall good levels of rigidity at the price of a mild global weight of the structure.
- *Nacelle*. The material of the nacelle may be the same as the load-bearing structure. The sides of the nacelle may be actually part of it. The structural role of the nacelle top is typically not relevant, hence this component can be manufactured from very light material.
- *Voltage booster*. As pointed out in section 3.1, this component is typically not to be found in powerplants for aviation, and its corresponding weight-to-power difference figure is rather penalizing, albeit already compatible with airship flight operations. Ways to obtain a better value of this parameter are currently under study.

The weight corresponding to ion-plasma thrusters can be related to their thrust, through a thrust-to-weight parameter $\frac{T}{W_m}$, which accounts for the aggregated contribution of all the components in the previous listing, except the voltage booster. This allows to define the weight of the propulsive units W_m from the knowledge of the top thrust gained from the analysis of the mission profile, whereas the weight W_{vb} of the voltage booster is typically computed separately, based on the power it has to deal with, which in turns is again related to the top thrust to be obtained from each thruster.
Concerning the sizing of the batteries, Eq. 3 is amended reflecting the fact that the propeller is not present any more, and conversely a figure of the power required from the electrical system for a given thrust is assigned through the parameter $\frac{T}{P_m}$. Therefore, the power absorbed by the thrusters and required from the batteries can be computed from the thrust directly as

$$P_m = \frac{T}{\left(\frac{T}{P_m}\right)}, \tag{11}$$

wherein thrust T on top represents the actual value of required thrust along the profile. The energy E can be obtained correspondingly, from the integration of the power required P_m along the mission. Based on this, the weight corresponding to the batteries can be computed according to the most stringent requirement among energy and power required (qualitatively similar to Eq. 3), as

$$W_{bat} = \frac{1}{\eta_d} \max\left(\frac{E}{e_{bat}}, \frac{P_m}{p_{bat}}\right). \tag{12}$$

The weight break-down in Eq. 5 can be therefore built up according to a modified set of components, as

$$W = W_{env} + W_{lg} + W_{bat} + W_m + W_{el} + W_{vb} + W_{gon} + W_{str} + W_t + W_{pl}, \tag{13}$$

wherein it should be observed that the weight of the batteries will be now computed from Eq. 12, and the weight of the gondola W_{gon} can be obtained as a function of the weight of the voltage booster W_{vb}, as well as of the other components stored in the gondola according to the baseline architecture (see section 2.1.2).
It is relevant to remark that the solution obtained from the sizing procedure just outlined is totally dependent on the many assumptions on the geometrical and technological features of the thruster (as specified in section 3.2.1). For this reason, an evaluation of the sensitivity of the outcome of the design procedure with respect to these parameters is of great interest, and it will be assessed in the application section 4.

4. Application studies

The sizing procedure introduced in this work, albeit rather generic, hence potentially capable of coping in particular with diverse target missions, has been employed here in conjunction with that of a low-altitude airship with no payload. This mission is of special interest, since the set up of an outdoor flying demonstrator pushed by ion-plasma thrusters is among the milestones of project `IPROP`.
In order to start the lofting and detailed design of the demonstrator, the outcome of the design procedure presented herein is of great use, allowing to obtain realistic basic data on airship sizing, accounting for the specific characteristics of the thrusters and components under development within the project.
The inclusion of this sizing procedure including ion-plasma thrusters as an option within the suite `Morning Star` [8, 11] has been carried out, and the optimal approach already implemented in that procedure for a conventionally-propelled airship has been employed to explore the space of design solutions. The results presented in this section show not only the weight break-down and characteristics of some realistic sizing solution, but also a wider study of the expected change of a weight-optimal solution with respect to a set of parameters. These parameters have been chosen within three groups:

1. Mission parameters. Among the parameters defining the demonstration mission are its endurance and target velocity. The latter can be intended as a telemetry (i.e. ground) velocity in still air, or similarly as a relative velocity in presence of wind.

2. Technology parameters not related to the thrusters. These include the energy and power density of the batteries, related by the chemistry of the battery itself, as well as the density of the envelope material.

3. Technology parameters related to the thrusters. These include the thrust-to-frontal area and thrust-to-power ratios of ion-plasma thrusters, as well as the weight of the voltage booster versus the power going through this component.

Additionally, we will investigate the effect of the number of thrusters, within a row and in terms of longitudinal arrangement, considering all technological parameters and mission specifications as assigned.
The baseline mission profile has been specified according to the planned location of the demonstration flight campaign, and the corresponding parameters are specified in Tab. 1.

Table 1 – Basic data for demonstration mission sizing.

Mission parameter	Value
Flight time	45 min
Climb and cruise velocity	3 m/s
Top altitude (above ground)	5 m
Climb and descent angle (absolute value)	30 deg

The cruise range is defined according to the specification of velocity and flight time.
As a baseline for the analyses to follow, some technological parameters have been set to reference values. These quantities are shown in Tab. 2.

Table 2 – Assigned values of technological parameters.

Component	Technological parameter	Value
Envelope	Surface density	250 g/m^2
	Maximum tensile strength	873 N/cm
Battery	Energy density	150 Wh/kg
	Power density	6,750 W/kg
	Charge/Discharge efficiency	80%
Cables	Volumetric density	8,960 kg/m^3

Unless differently specified, values in Tab. 2 have been considered for the corresponding parameters in the analyses to follow.
Care has been taken to avoid non-standard technology as far as possible, and correspondingly optimistic assumptions on performance. Data of materials currently employed by partners within project IPROP have been selected. Concerning the envelope material, data in Tab. 2 refer to a typical polyurethane for airship construction. Battery technology data refer to off-the-shelf products based on Lithium-Polymer chemistry. Electric cables are manufactured from standard copper wires.
Additional parameters specific to the propulsive technology considered in the analyses will be shown in the pertinent paragraphs below.

4.1 Comparison of design solutions based on conventional vs. ion-plasma thrusters

The design methodology outlined in the previous paragraphs has been applied to the design of the demonstrator introduced earlier in section 4. In order to show the effectiveness and to assess the feasibility of the ion-plasma thruster solution with respect to a baseline, two concurrent designs have been carried out.
Firstly, the demonstrator has been sized based on a standard propulsion technique, employing electric motors and propellers. In this case, the sizing of the propulsion system requires the definition of a technological relationship between the power needed for propulsion and the weight of the motor, so as to define W_m in Eq. 5 based on the value of required power $P_{r,\max}$ resulting from the mission. In particular, a linear relationship based on off-the-shelf motors for flying models of comparable power required as the airship demonstrator at hand has been employed, yielding $\frac{P_{r,\max} g}{W_m} = 90$ W/kg. Furthermore, as required according to Eq. 3, values of the propeller and motor efficiency respectively of $\eta_P = 80\%$ and $\eta_m = 90\%$ have been assumed.
Secondly, the demonstrator has been sized employing ion-thrusters instead of standard electromechanical propulsion. Since in this case the number of thrusters on board influences the outcome of the sizing (see section 3.2.2), it is assumed to mount $N_t = 9$ thrusters, arranged in $N_l = 3$ longitudinally-placed rows of $N_{t,l} = 3$ radially-placed thrusters each. The geometry of each thruster is assigned as required by the sizing procedure in terms of length $l = 0.045$ m and height $h = 0.125$ m. The density of the collectors within the ion-plasma thrusters has been assumed of 1,079 kg/m^3, from experiments on prototypes developed within the activities of project IPROP, and corresponding to filled structures mostly made of 3D-printable material. A 50% infill allows to actually reduce this figure by the same amount, without apparently producing any detrimental effect on structural stiffness. The density of the external structure of the thruster is assumed of 50 kg/m^3, which corresponds to standard styrofoam. It has been practically checked that a load-bearing structure made of this material, where suitably lofted, allows to support the range of loads to which the thruster should be subjected on the demonstrator. Correspondingly, the thrust-to-power ratio has been set to $\frac{T}{P_m} = 5.2$ 1/s, and the thrust-to-area ratio of the ion-plasma thrusters to an experimentally feasible value of $\frac{T}{A_m} = 4.23$ N/m^2. Both reflect practically attainable results from laboratory testing campaigns within IPROP. Finally, a currently achievable value of $\frac{W_{vb}}{P_m} = 0.83$ kg/kW has been assumed for the voltage booster.

The results of the weight-optimal sizing for the demonstrator airship, obtained assuming a conventional and ion-plasma thruster propulsion respectively, are displayed in Tab. 3. For both designs, the limit tensile strength $\bar{\sigma}_{\max}$ in Eq. 6 has been set to 873 N/cm, and the limit buoyancy ratio BR in Eq. 7 to 0.95.

Table 3 – Results of weight optimal sizing for the airship demonstrator. Conventional and ion-plasma thrusters. Baseline technology data assumed for the computations.

Quantity	Conventional thrusters	Ion-plasma thrusters
Envelope length L_r [m]	5.52	8.06
Fineness ratio FR	3.73	3.00
Total weight W [kg]	6.87	33.14
Envelope weight W_{env} [kg]	6.23	16.72
Lifting gas weight W_{lg} [kg]	1.21	5.05
Support structures, tail weight $W_{str}+W_t$ [kg]	0.47	1.55
Thruster weight W_m+W_{el} [kg]	0.12	1.28
Voltage booster W_{vb} [kg]	0	0.71
Battery weight W_{bat} [kg]	0.035	5.89

From the analysis of the results in Tab. 3, it is apparent how the results in terms of overall sizing are pretty different. Both design are relatively compact and generally feasible in practice, yet the length of the airship propelled by the ion-plasma thruster is somewhat bigger than that of a corresponding conventionally-propelled machine. The main weight component producing this difference is that of the thruster system, mainly composed of the thruster and voltage booster. The limited thrust-to-power of the thrusters (a measure of energetic efficiency), and the addition of the voltage booster with respect to the conventional case, provoke an increase in the volume of the envelope for a better lifting ability. This in turns imposes a more penalizing geometrical and weight sizing of the machine in its structural part, which raises drag and produces the need for an increased thrust, hence the need for bigger thrusters and batteries. As previously noted, the development of more performing voltage boosters is among the expected key findings of project `IPROP`, together with the development of the ion-plasma thrusters themselves.

4.2 Effect of mission and technological parameters on the design solution

The design solution obtained from the optimal sizing procedure in section 4.1 shows that a significant difference exists between an airship sized considering conventional thrusters and that obtained from ion-plasma thrusters. As anticipated, it is interesting to investigate the sensitivity of the design solution obtained when the novel ion-plasma thrusters are mounted on board, and corresponding to changing values of some parameters either pertaining to the mission or bound to technological assumptions.

4.2.1 Effect of mission parameters

The plot in Fig. 4 shows the breakdown of the weights obtained perturbing the target endurance of the mission, for an airship based on ion-plasma thrusters. In particular, the propulsion system is the component where the thrusters and the voltage booster are wrapped. It is immediately evident how the trend on overall weight is roughly linear, with a significant impact on battery weight, as expected, driving the increase in the general sizing, hence in particular the weight of the envelope.
Another interesting effect is that of target velocity. Both plots in Fig. 5 show the result on the weight breakdown due to an increase in cruise velocity. The velocity domain has been split on the two plots, on account of the fact that up to a velocity of 3 m/s (left plot) it was found that the width w of the thrusters could solve the loop described in section 3.2.2 thus coping with the required thrust-to-area ratio $\frac{T}{A_m}$ imposed as a parameter, whereas this was not possible over that velocity (right plot). In order to solve the equivalence between $\left(\frac{T}{A_m}\right)_{req}$ and $\frac{T}{A_m}$ over 3 m/s, an increase in the height s of each thruster was required, which in technological terms corresponds to the adoption of a larger number of emitters and collectors within the ion-plasma thruster. In particular, where a number of

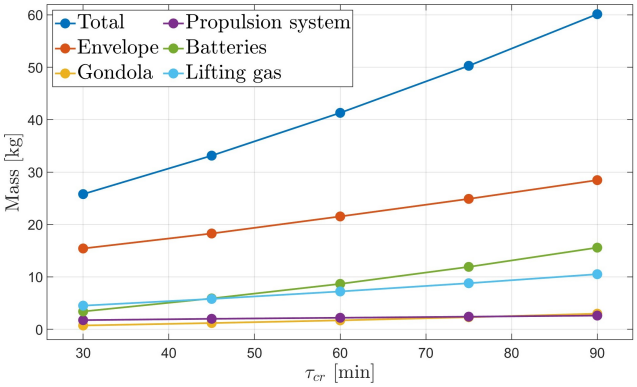

Figure 4 – Effect of a change in target mission endurance on the weight breakdown of an airship demonstrator featuring ion-plasma thrusters.

these couples of 4 is sufficient up to 3 m/s, thus producing a width w from the sizing procedure which is not geometrically excessive, in order to obtain the same result at higher velocity values the number of emitters and collectors has been raised to 8 and 12 respectively for 4 and 5 m/s. The increase in the number of couples is reflected by the increase in s, as said, and in turn in the ability of the sizing algorithm to preserve the equivalence $\left(\frac{T}{A_m}\right)_{req}$ vs. $\frac{T}{A_m}$ through a lower width w, compatible with the curvature and overall width of the airship envelope, where the thrusters are strapped.

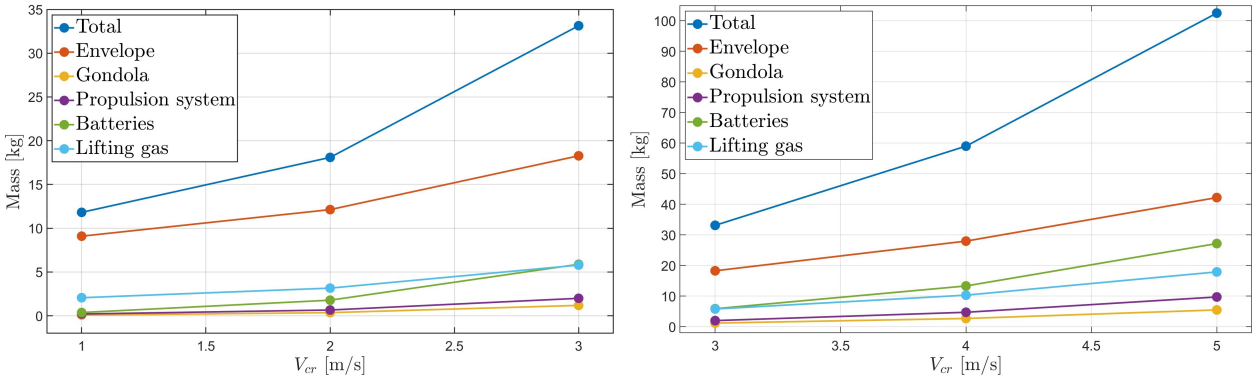

Figure 5 – Effect of a change in target cruise velocity on the weight breakdown of an airship demonstrator featuring ion-plasma thrusters. Left: number of collectors is 4. Right: number of collectors is respectively 4, 8, 12 for increasing values of nodal velocity.

It is interesting to note that further variables have been investigated, contributing to the definition of the mission profile. These include the temperature of the air, tested between 0 and 40° C (the reference value being the standard temperature of 15° C), and the target altitude of the cruise phase, tested between 5 and 15 m. Both ranges have been selected on account of the specific target mission (i.e. a low altitude demonstrator), and are therefore not general. However, the effect of such changes has been found to be totally negligible in the case at hand (i.e. no significant alteration of the overall weight nor of the breakdown have been observed).

4.2.2 Effect of technology parameters not related to ion-plasma thrusters

As typical for flying machines featuring a battery-based propulsion system [21, 22], since the energy storage system takes a significant share of the overall weight of the machine, it is typical to observe a certain sensitivity of the overall weight when the technological parameters pertaining to the battery are altered.

The plot in Fig. 6 shows the breakdown of the weights obtained by changing the values of the energy density e_{bat} of the batteries. Values of these parameters are kept within a certain range, so as to remain within the feasible performance of Lithium-Polymer chemistry.

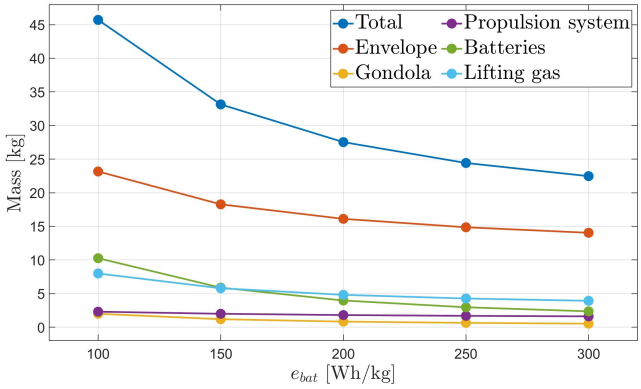

Figure 6 – Effect of a change in the specific energy of the battery on the weight breakdown of an airship demonstrator featuring ion-plasma thrusters.

It is interesting to note that the change in the overall weight is significantly non-linear, by coincidence, especially to the left of the reference value of $e_{bat} = 150$ Wh/kg. This means that a reduction in the energy density of the batteries below the assumed reference value would be extremely penalizing, whereas a progressively more limited advantage can be expected by pushing the energy density up. In particular, this is due to the little effect of this parameter on the weight of the propulsion system and voltage booster (in the propulsion system).
Differently from the case of heavier-than-air craft (e.g. aircraft or multi-copters), typically encountering stark power requirements from the take-off and climb maneuvers, which in turns make the specific power of the battery sometimes more constraining than specific energy, it can be observed that for the airship at hand the specific energy of the battery makes for a harder constraint, irrespective of the change in specific power considered in this work. This is on the one hand inherent to lighter-than-air craft, since buoyancy allows a significant reduction of the thrust or power requirement put on the thrusters in take-off and climb. On the other, the demonstration mission considered here, featuring a low cruising level above ground (see Tab. 1), increases this effect further.
Another interesting effect not related to the specific features of ion-plasma thrusters is obtained when changing the density of the envelope material. From Fig. 7, it is possible to notice that the sensitivity of the overall weight on this parameter is generally high, with significant changes in the result for slight changes in the density of the material. Furthermore, the behavior is non-linear, with a ramp-up of the sensitivity not far to the right of the reference value of 250 g/m^2.

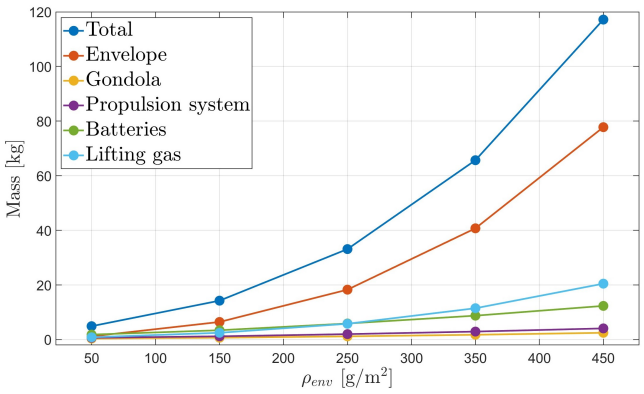

Figure 7 – Effect of a change in the envelope material density on the weight breakdown of an airship demonstrator featuring ion-plasma thrusters.

4.2.3 Effect of technology parameters bound to ion-plasma thrusters

A further batch of analyses is that related to the sensitivity to parameters pertaining to the ion-plasma thrusters. In Fig. 8 it is possible to note how the effect of the weight-to-power ratio of the voltage

booster is basically linear on the overall weight, and how it produces a relatively limited absolute change on that weight, at least for the considered range of values of this technological parameter, and compared for instance to the density of the envelope (Fig. 7).

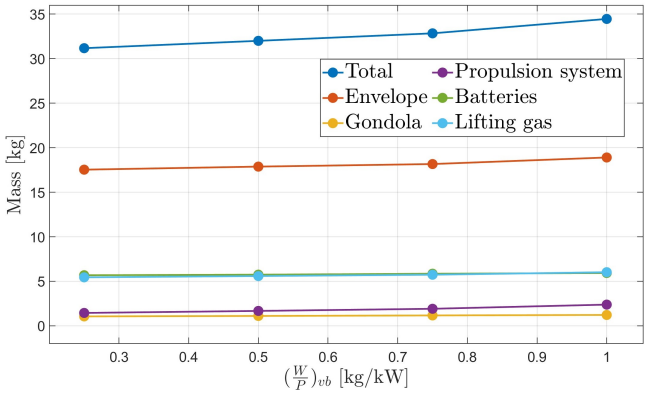

Figure 8 – Effect of a change in the weight-to-power ratio of the voltage booster on the weight breakdown of an airship demonstrator featuring ion-plasma thrusters.

This result is possibly bound to the relatively limited values of power involved in the propulsion system, which is a typical feature of airships compared to fixed-wing aircraft or rotorcraft.
The plots in Fig. 9 refer to parameters eminently bound to the technology of the ion-plasma thrusters under development. The effects of thrust-to-area ratio $\frac{T}{A_m}$ (left) and thrust-to-power ratio $\frac{T}{P_m}$ (right) are displayed. It can be observed that the effect of both parameters, which should be increased to obtain a more performing thruster, is generally non-linear on the overall weight. In particular, for the considered reference values of the two parameters, the sensitivity is generally high, suggesting that even a slight improvement on these parameters from that value may imply a significant gain in terms of weight.

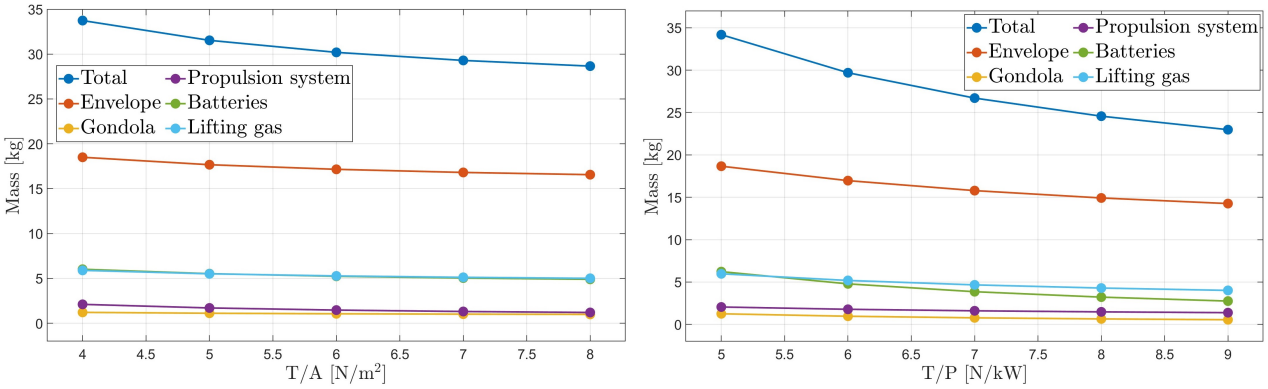

Figure 9 – Effect of a change in the thrust-to-area (left) and thrust-to-power ratio (right) of the ion-plasma thrusters on the weight breakdown of an airship demonstrator.

Finally, considering the fact that ion-plasma thrusters are arranged in radial and in longitudinal arrays, it is interesting to analyze the effect of the parceling of thrust on a different set and arrangement of the thrusters. This corresponds to the parameterized change in the values of the numbers of longitudinal stations N_l, and of the thrusters per station $N_{t,l}$. The plots in Fig. 10 show the result of optimal sizing with different assignments of these parameters. On the left and right plots are reported the length L_r and the weight W respectively. The fineness ratio FR is not changing in this result, since it is constantly set to its minimum value of $FR = 3.0$, set in the optimal seek procedure for reasons bound to aerodynamic shaping and technological manufacture of the envelope (however, it has been checked that the effect of these parameters on the optimal fineness ratio is generally more negligible even if the latter is left free to change, in particular producing a slightly slenderer envelope for higher values of the both N_l and $N_{t,l}$).

From the top plots, it can be observed that an increase in both parameters, resulting in a higher number of thrusters N_t, produces a mild increase of the optimal length L_r (which comparing the far ends of the spectrum is approximately 10%).

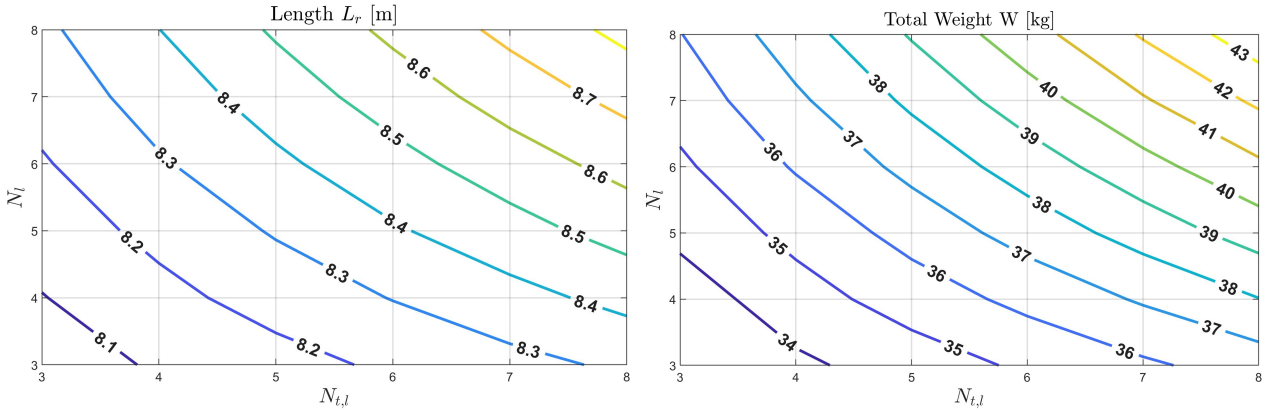

Figure 10 – Optimally sized values of airship length L_r (left) and weight W (right) for different values of the sizing parameters N_l and $N_{t,l}$.

Conversely, the bottom plot in Fig. 10 displays a more significant effect on the overall weight W (with a maximum change of more than 20%, based on the considered range of the parameters), and features an increase of the result when increasing the values of both N_l and $N_{t,l}$. This behavior can be explained by the increase in drag associated with the increase in the number of thrusters, and the ensuing required increase in required thrust hence general sizing of the machine. Therefore, it can be argued that a more reduced number of thrusters has a beneficial effect on both weight and geometrical sizing, even though the absolute changes involved in association to a change in N_l and $N_{t,l}$ are in any case not dramatic.

5. Conclusions

The present contribution has introduced an amendment to an original preliminary sizing algorithm for airships, originally developed by the authors considering electro-mechanical motors, such to cope with ion-plasma thrusters, under development within project `IPROP`. The so-identified procedure allows to keep the number of free sizing parameters to a minimum, while coping with the specific features of this novel type of thrusters, and making use of the technological data pertaining to them as obtained from experiments. The sizing algorithm, which works in an automated fashion within the airship sizing suite `Morning Star`, returns a general sizing of the envelope, weight break-down and propulsive system, based on a weight-optimal criterion and complying with constraints coming from the mission profile and from technological limits.

Preliminary sizing results for the design of a low-altitude technological demonstrator, among the milestones of project `IPROP`, show that an airship based on ion-plasma thrusters is indeed feasible at the current technological level, albeit in association with a slightly more requiring sizing solution compared to a case based on standard propulsion.

An exploration of the space of design solutions has been carried out, considering changing values of the parameters pertaining to the mission profile, as well as technological parameters related to the subsystems on board the airship, including ion-plasma thrusters. Comapared to technological features pertaining to the envelope material, the effect of battery and thruster-related technological features appear to influence the result to a milder (albeit in any case sizeable) extent, highlighting the relevance of the choice of the material on the absolute values obtained from a weight-optimal sizing.

A study of the arrangement of the ion-plasma thrusters on board (which still does not account for any implication on the dynamic behavior of the airship and its controllability, to be assessed through further research within project `IPROP`) has shown that a significant effect on mass can be expected, under the adopted assumptions on the distribution of thrust and drag among the thrusters, when the number of thrusters is increased. This suggests that the adoption of a lower number of thrusters with

a higher nominal thrust may induce a better weight performance compared to a higher number of less capable, smaller thrusters.
Further research on design will follow suit within `IPROP`, especially studying the applicability of an airship concept based on ion-plasma thrusters to the case of a stratospheric airship, and adding considerations on optimality bound to detailed lofting of the weight components onboard, which invariably bear an effect on dynamic performance and controllability.

6. Contact Author Email Address

Questions and queries concerning this research should be addressed to Prof. Carlo E.D. Riboldi (carlo.riboldi@polimi.it) and Prof. Marco Belan (marco.belan@polimi.it).

7. Copyright Statement

8. Acknowledgements

This project has received funding from the European Union under grant agreement No.101098900, within the European Innovation Council (EIC) Pathfinder Open programme of 2022 (call HORIZON EIC 2022 PATHFINDEROPEN 01).

9. Disclaimer

The content of this document reflects only the author's view. The European Commission is not responsible for any use that may be made of the information it contains.

References

[1] G. Romeo, G. Frulla, and E. Cestino. Design of a high-altitude long-endurance solar-powered unmanned air vehicle for multi-payload and operations. *Journal of Aerospace Engineering*, 221:199–216, 2007.

[2] S. Smith, M. Fortenberry, M. Lee, and R. Judy. HiSentinel80: Flight of a High Altitude Airship. In *11th AIAA Aviation Technology, Integration, and Operations (ATIO) Conference, 20-22 September 2011, Virginia Beach, VA*, 2011.

[3] J. Gonzalo, D. López, D. Domínguez, A. García, and A. Escapa. On the capabilities and limitations of high altitude pseudo-satellites. *Progress in Aerospace Sciences*, 98:37–56, 2018.

[4] Kelluu Oy, Metallimiehentie 4, 80330 Reijola, Finland, 2023.

[5] D. P. Raymer. *Aircraft Design: a Conceptual Approach*. AIAA Education Series. American Institute of Aeronautics and Astronautics, Washington, D.C., third edition edition, 1999.

[6] A. Colozza. Initial Feasibility Assessment of a High Altitude Long Endurance Airship. Technical Report NASA/CR–2003-212724, Analex Corp., 2003.

[7] G. E. Carichner and L. M. Nicolai. *Fundamentals of Aircraft and Airship Design*. AIAA Education Series. American Institute of Aeronautics and Astronautics, Inc., 2013.

[8] C. E. D. Riboldi, A. Rolando, and G. Regazzoni. On the feasibility of a launcher-deployable high-altitude airship: Effects of design constraints in an optimal sizing framework. *Aerospace*, 9:1–37, 2022.

[9] P. Lobner. HiSentinel Stratospheric Airships. Technical report, Lyncean Group of San Diego, 2020.

[10] I. S. Smith. Hisentinel & stratospheric airship design sensitivity. In *Keck Institute for Space Studies (KISS) Workshop, 30 April-3 May 2013, Pasadena, CA*, 2013.

[11] C. E. D. Riboldi, A. Rolando, S. Cacciola, G. Regazzoni, and I. Spadafora. On the Optimal Preliminary Design of High-Altitude Airships: Automated Procedure and the Effect of Constraints. In *Aerospace Europe Conference 2023 - 10th EUCASS - 9th CEAS, 9-13 July 2023, Lausanne, Switzerland*, 2023.

[12] C. E. D. Riboldi and A. Rolando. Layout Analysis and Optimization of Airships with Thrust-Based Stability Augmentation. *Aerospace*, 9:393, 2022.

[13] C. E. D. Riboldi and A. Rolando. Thrust-based stabilization and guidance for airships without thrust-vectoring. *Aerospace*, 10, 2023.

[14] C. E. D. Riboldi and A. Rolando. Autonomous flight in near hover and hover for thrust controlled unmanned airships. *Drones*, 7, 2023.

[15] M. Belan, L. Arosti, R. Polatti, F. Maggi, S. Fiorini, and F. Sottovia. A parametric study of electrodes geometries for atmospheric electrohydrodynamic propulsion. *Journal of Electrostatics*, 113:103616, 2021.

[16] M. Belan, R. Terenzi, S. Trovato, and D. Usuelli. Effects of the emitters density on the performance of an atmospheric ionic thruster. *Journal of Electrostatics*, 120:103767, 2022.

[17] O. Kahol, M. Belan, M. Pacchiani, and D. Montenero. Scaling relations for the geometry of wire-to-airfoil atmospheric ionic thrusters. *Journal of Electrostatics*, 123:103815, 2023.

[18] A. Brown, H. Xu, C. K. Gilmore, and S. R. H. Barrett. Solid-state electroaerodynamic aircraft design using signomial programming. *Journal of Aircraft*, 61(1):280–290, 2024.

[19] HORIZON-EIC-2022-PATHFINDEROPEN-01. Ionic propulsion in the atmosphere, 2023.

[20] X. Yang and D. Liu. Conceptual design of stratospheric airships focusing on energy balance. *Journal of Aerospace Engineering*, 31, 2018.

[21] C. E. D. Riboldi and F. Gualdoni. An integrated approach to the preliminary weight sizing of small electric aircraft. *Aerospace Science and Technology*, 58:134–149, 2016.

[22] C. E. D. Riboldi. An optimal approach to the preliminary design of small hybrid-electric aircraft. *Aerospace Science and Technology*, 81:14–31, 2018.

[23] C. E. D. Riboldi. Energy-optimal off-design power management of hybrid-electric aircraft. *Aerospace Science and Technology*, 95:1–16, 2019.

[24] M. M. Munk. The aerodynamic forces on airship hulls. Technical report, NACA, 1926. National Advisory Committee for Aeronautics, Report No.184.

[25] N. Gomez-Vega, A. Brown, H. Xu, and S. R. H. Barrett. Model of multistaged ducted thrusters for high-thrust-density electroaerodynamic propulsion. *AIAA Journal*, 61(2):767–779, 2023.

[26] N. Gomez-Vega and S. R. H. Barrett. Order-of-magnitude improvement in electroaerodynamic thrust density with multistaged ducted thrusters. *AIAA Journal*, 62(4):1342–1353, 2024.